Article

Fluorine Substituted Adenosines As Probes of Nucleobase Protonation in Functional RNAs

Ian T. Suydam, and Scott A. Strobel

J. Am. Chem. Soc., **2008**, 130 (41), 13639-13648 • DOI: 10.1021/ja803336y • Publication Date (Web): 20 September 2008

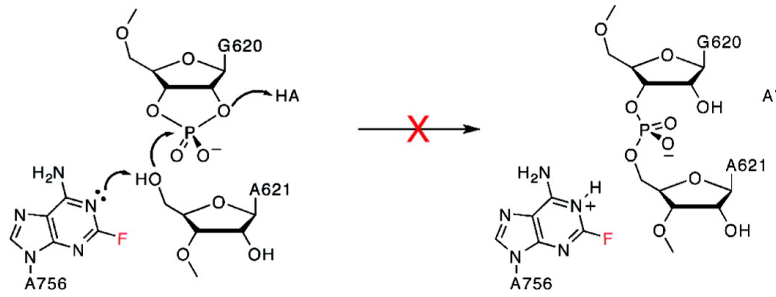

More About This Article

Additional resources and features associated with this article are available within the HTML version:

- Supporting Information
- Access to high resolution figures
- Links to articles and content related to this article
- Copyright permission to reproduce figures and/or text from this article

View the Full Text HTML

J|A|C|S
ARTICLES

Published on Web 09/20/2008

Fluorine Substituted Adenosines As Probes of Nucleobase Protonation in Functional RNAs

Ian T. Suydam and Scott A. Strobel*

Department of Molecular Biophysics and Biochemistry and Department of Chemistry, Yale University, 260 Whitney Avenue, New Haven, Connecticut 06520-8114

Received May 5, 2008; E-mail: scott.strobel@yale.edu

Abstract: Ionized nucleobases are required for folding, conformational switching, or catalysis in a number of functional RNAs. A common strategy to study these sites employs nucleoside analogues with perturbed pK_a, but the interpretation of these studies is often complicated by the chemical modification introduced, in particular modifications that add, remove, or translocate hydrogen bonding groups in addition to perturbing pK_a values. In the present study we present a series of fluorine substituted adenosine analogues that produce large changes in N1 pK_a values with minimal structural perturbation. These analogues include fluorine for hydrogen substitutions in the adenine ring of adenosine and 7-deaza-adenosine with resulting N1 pK_a values spanning more than 4 pK_a units. To demonstrate the utility of these analogues we have conducted a nucleotide analogue interference mapping (NAIM) study on a self-ligating construct of the Varkud Satellite (VS) ribozyme. We find that each of the analogues is readily incorporated by T7 RNA polymerase and produces fully active transcripts when substituted at the majority of sites. Strong interferences are observed for three sites known to be critical for VS ribozyme function, most notably A756. Substitutions at A756 lead to slight enhancements in activity for elevated pK_a analogues and dramatic interferences in activity for reduced pK_a analogues, supporting the proposed catalytic role for this base. The structural similarity of these analogues, combined with their even incorporation and selective interference, provides an improved method for identifying sites of adenosine protonation in a variety of systems.

Introduction

Ribonucleic acids are increasingly found to be involved in a wide variety of cellular functions outside their traditionally accepted roles in protein translation, where they act as information carriers (mRNA), decoding elements (tRNA), or ribosomal constituents (rRNA). These functions include RNA splicing,[1] tRNA maturation,[2] plasmid replication,[3] and gene regulation, either through metabolite binding[4] or via a number of RNA mediated gene silencing pathways.[5] Many of these functions require RNA sequences capable of adopting well-defined folds, and in some cases these folds produce active sites capable of catalysis, most commonly the breakdown or formation of phosphodiester bonds, either at a defined site within the structured RNA itself or in some external substrate RNA sequence. These RNA based enzymes, or ribozymes, were originally thought to exist exclusively as metalloenzymes, employing positioned divalent cations in their active sites to catalyze phosphodiester transfer reactions.[6] However, a number of nucleolytic ribozymes, which produce free 5′-hydroxyl and 2′,3′-cyclic phosphates as cleavage products, have been shown to be functional in the absence of divalent metals.[7] These results in combination with pH profiles of reaction rate and an increasing number of crystal structures showing appropriate geometries suggest some ribozymes may be capable of general acid/base catalysis, with the nucleobases themselves acting as the site of proton transfer.[8−10] In these systems the active site nucleobases are predicted to perform a role analogous to that of histidines in protein ribonucleases.[11]

General acid/base mechanisms for ribozyme catalyzed reactions require substantial pK_a perturbations. The RNA functional groups with unperturbed pK_a values closest to neutrality are the nitrogens of nucleobase heterocycles, namely N3 of cytidine (pK_a = 4.2), N1 of adenosine (pK_a = 3.5), N1 of guanosine (pK_a = 9.2), and N3 of uridine (pK_a = 9.2).[10] Because ribozymes are folded polyanions, the stabilization of the protonated forms of bases, leading to elevation in pK_a values, is expected to be favored. This stabilization makes cytidine and adenosine attractive candidates for sites of proton transfer. Elevated pK_a values for these bases have been observed with

(1) Kruger, K.; Grabowski, P. J.; Zaug, A. J.; Sands, J.; Gottschling, D. E.; Cech, T. R. *Cell* **1982**, *31*, 147–157.
(2) Guerriertakada, C.; Gardiner, K.; Marsh, T.; Pace, N.; Altman, S. *Cell* **1983**, *35*, 849–857.
(3) Kennell, J. C.; Saville, B. J.; Mohr, S.; Kuiper, M. T. R.; Sabourin, J. R.; Collins, R. A.; Lambowitz, A. M. *Genes Dev.* **1995**, *9*, 294–303.
(4) Mandal, M.; Breaker, R. R. *Nat. Rev. Mol. Cell Biol.* **2004**, *5*, 451–463.
(5) Hannon, G. J. *Nature* **2002**, *418*, 244–251.
(6) Pyle, A. M. *Science* **1993**, *261*, 709–714.
(7) Murray, J. B.; Seyhan, A. A.; Walter, N. G.; Burke, J. M.; Scott, W. G. *Chem. Biol.* **1998**, *5*, 587–595.
(8) Das, S. R.; Piccirilli, J. A. *Nat. Chem. Biol.* **2005**, *1*, 45–52.
(9) Nakano, S.; Chadalavada, D. M.; Bevilacqua, P. C. *Science* **2000**, *287*, 1493–1497.
(10) Bevilacqua, P. C.; Brown, T. S.; Nakano, S.; Yajima, R. *Biopolymers* **2004**, *73*, 90–109.
(11) Raines, R. T. *Chem. Rev.* **1998**, *98*, 1045–1065.

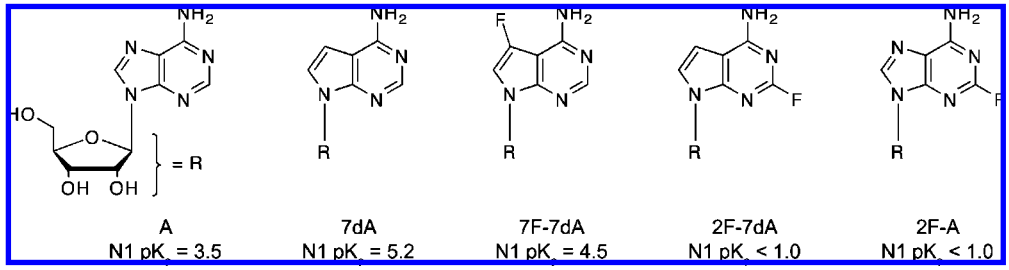

Figure 1. pK_a perturbed adenosine analogues.

spectroscopic techniques in a number of systems,[12−17] and calculations suggest these shifts arise from a combination of noncanonical base pairing interactions and focused electrostatic potentials arising from the phosphate backbone.[18]

While spectroscopic techniques provide an important tool for identifying sites of pK_a perturbation, they provide no information on the functional consequence of protonation at these sites. This is of particular concern when truncated or stabilized versions of the system are required, as is often the case in NMR studies, particularly those that investigate individual domains of the full ribozyme.[15,17] An alternative approach is to incorporate nucleotide analogues with a perturbed pK_a and to assay the effect of analogue substitution on catalysis. One challenge of this approach is the design of analogues that produce large changes in pK_a while maintaining other structural features, most notably hydrogen bonding patterns. Analogues must then be incorporated into the functional RNA in a manner that allows for a site-by-site evaluation of the effect on function. The most straightforward method of incorporation is to introduce analogues site specifically via oligonucleotide synthesis and to measure the effect on observed rates directly. The limitations of this strategy include the stability of the desired analogue to RNA synthesis conditions and the relatively short RNA sequences accessible by direct synthesis. Although longer RNA sequences can be reassembled through RNA ligations or alternative methods, the need to repeat this process for each site of interest often makes a complete analysis impractical.

Nucleotide analogue interference mapping (NAIM) provides a semiquantitative alternative to site specific incorporation. The NAIM method utilizes 5′-*O*-(1-thio)nucleotide triphosphates with an additional chemical modification in the ribose or nucleobase. Unlike synthetic methods, the analogues are incorporated by *in vitro* transcription, allowing any functional RNA transcript of virtually any length to be investigated. NAIM studies consist of four basic steps (for reviews of the NAIM method see refs 19 and 20). (i) Transcripts of the functional RNA are prepared where one of the four bases (A, U, G, or C) is substituted at low frequency with a nucleotide analogue. In this step the ratio of nucleotide triphosphate and analogue 5′-*O*-(1-thio)nucleotide triphosphate is adjusted such that any individual transcript contains approximately one analogue substitution at a random site. (ii) The active members of the transcribed pool are separated from the inactive members, most commonly by a change of electrophoretic mobility or a transfer of a radioisotope. (iii) The phosphorothioate linkage introduced at sites of analogue substitution is selectively cleaved by treatment with iodine. (iv) Sites of analogue interference are identified by separating the iodine cleaved RNAs by gel electrophoresis and quantitating relative band intensities by autoradiography. NAIM studies have successfully identified RNA functional groups required for catalysis, folding, or ligand binding in a number of systems.[21−25]

Identification of nucleobase protonation sites by NAIM requires a series of analogues with a perturbed pK_a. Previous studies investigating adenosine protonation have used analogues in one of two categories, those that make carbon/nitrogen substitutions in the adenine ring, including 3-deaza-adenosine (c^3A), 7-deaza-adenosine (7dA), Formycin (FormA), and 8-aza-adenosine (n^8A), and those that add, remove, or translocate the exocyclic amine, including 2,6-diaminopurine (DAP), purine (Pur), and 2-aminopurine (2AP).[21,23] Several of these analogues are incorporated with relatively poor efficiency by T7 RNA polymerase (c^3A, n^8A, Pur, 2AP),[20] others alter standard base pairing interactions (Pur, 2AP) or exist in multiple tautomeric forms (FormA).[26] To improve the identification of protonated adenosines in functional RNAs we set out to design a new series of structurally similar adenosine analogues that retain hydrogen bonding patterns on the Watson−Crick face of the base, are readily incorporated by T7 polymerase, and which produced large shifts in N1 pK_a values.

The analogues presented in this study make fluorine for hydrogen substitutions in adenosine or 7-deaza-adenosine (Figure 1). This series was chosen because the introduction of fluorine produces large pK_a shifts in nitrogen heterocycles with relatively modest structural perturbation.[27] Fluorine substitutions were introduced into adenosine at the 2-position (2F-A) and 7-deaza-adenosine at the 2- or 7-position (2F-7dA and 7F-7dA,

(12) Gong, B.; Chen, J. H.; Chase, E.; Chadalavada, D. M.; Yajima, R.; Golden, B. L.; Bevilacqua, P. C.; Carey, P. R. *J. Am. Chem. Soc.* **2007**, *129*, 13335–13342.
(13) Moody, E. M.; Brown, T. S.; Bevilacqua, P. C. *J. Am. Chem. Soc.* **2004**, *126*, 10200–10201.
(14) Legault, P.; Pardi, A. *J. Am. Chem. Soc.* **1997**, *119*, 6621–6628.
(15) Ravindranathan, S.; Butcher, S. E.; Feigon, J. *Biochemistry* **2000**, *39*, 16026–16032.
(16) Luptak, A.; Ferre-D'Amare, A. R.; Zhou, K. H.; Zilm, K. W.; Doudna, J. A. *J. Am. Chem. Soc.* **2001**, *123*, 8447–8452.
(17) Flinders, J.; Dieckmann, T. *J. Mol. Biol.* **2001**, *308*, 665–679.
(18) Tang, C. L.; Alexov, E.; Pyle, A. M.; Honig, B. *J. Mol. Biol.* **2007**, *366*, 1475–1496.
(19) Ryder, S. P.; Ortoleva-Donnelly, L.; Kosek, A. B.; Strobel, S. A. *Methods Enzymol.* **2000**, *317*, 92–109.
(20) Cochrane, J. C.; Strobel, S. A. *Current Protocols in Nucleic Acid Chemistry*; Wiley: New York, 2004; *Vol. 2*.
(21) Jones, F. D.; Strobel, S. A. *Biochemistry* **2003**, *42*, 4265–4276.
(22) Oyelere, A. K.; Kardon, J. R.; Strobel, S. A. *Biochemistry* **2002**, *41*, 3667–3675.
(23) Ryder, S. P.; Oyelere, A. K.; Padilla, J. L.; Klostermeier, D.; Millar, D. P.; Strobel, S. A. *RNA* **2001**, *7*, 1454–1463.
(24) Szewczak, A. A.; Ortoleva-Donnelly, L.; Zivarts, M. V.; Oyelere, A. K.; Kazantsev, A. V.; Strobel, S. A. *Proc. Natl. Acad. Sci. U.S.A.* **1999**, *96*, 11183–11188.
(25) Kwon, M. Y.; Strobel, S. A. *RNA* **2008**, *14*, 25–34.
(26) Kierdaszuk, B.; Modrak-Wojcik, A.; Wierzchowski, J.; Shugar, D. *Biochim. Biophys. Acta, Protein Struct. M.* **2000**, *1476*, 109–128.
(27) Perrin, D. D. *Dissociation Constants of Organic Bases in Aqueous Solution*; Butterworths: London, 1965.

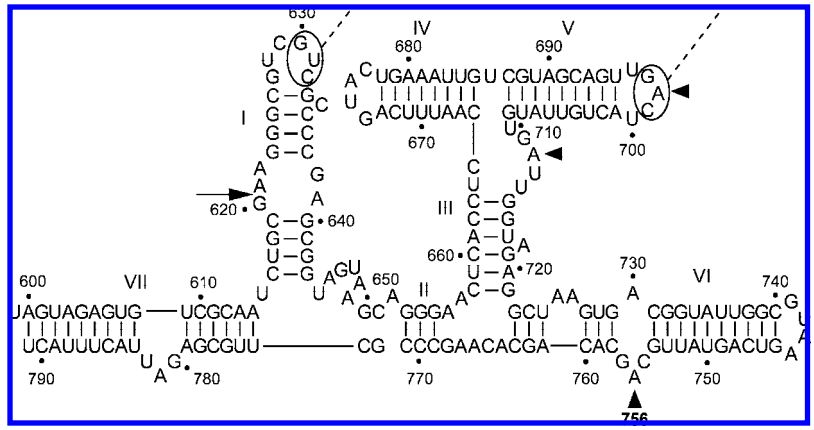

Figure 2. Predicted secondary structure of the VSE ribozyme (VS RNA NT 599−791 containing point mutants A782U and U785C). Helices are numbered I−VII, with the site of ligation marked with the arrow, and the tertiary "kissing" interaction shown with the dashed line. The unligated VSE RNA (NT 621−791) was transcribed with analogues **7a**−**7e** randomly incorporated, and the substrate RNA (NT 599−620) was prepared with a 2′,3′-cyclic phosphate terminus. The NAIM analysis assayed the effect of analogue substitution from A645 to A767. Sites of interference with at least one analogue are denoted with filled triangles.

Scheme 1[a]

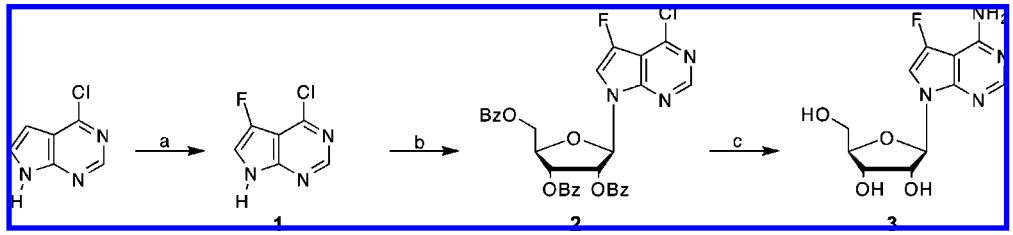

[a] (a) Selectfluor, CH_3CN, acetic acid, 70 °C 15 h. (b) BSA, CH_3CN, 1-*O*-acetyl-2,3,5-tri-*O*-benzoyl-*β*-D-ribofuranose, TMSOTf, 80 °C 1 h. (c) NH_3/MeOH, 73 °C 18 h.

Figure 1). These structurally similar analogues have N1 pK_a values spanning more than 4 pK_a units and are readily incorporated by T7 RNA polymerase (see below). Importantly, all five members of the series retain the exocyclic amine for standard base pairing interactions.

To demonstrate the utility of this new series of adenosine analogues we conducted a NAIM study on a ligating form of the Varkud Satellite (VS) ribozyme[21,28] (Figure 2). We chose to study a ligating form of the VS ribozyme because less information is currently available for the VS catalyzed reaction in the direction of ligation than in the direction of cleavage. The ligation of a radiolabeled substrate also provides a straightforward functional selection, which simplifies the NAIM experiment. The role of A756 is of particular interest since this nucleotide has been proposed as a site of proton transfer in the cleavage reaction.[29−31] A previous NAIM study on this construct using the analogues Pur, n^8A, FormA, and 7dA observed an interference pattern consistent with A756 protonation, but these analogues also produced a number of interferences at other sites that were less easily interpreted.[21] We set out to confirm the importance of A756 protonation with a distinct class of pK_a perturbed analogues and to see if the structural similarity of these analogues would produce a more selective and interpretable interference pattern.

Results

Synthesis. 7-Fluoro-7-deaza-adenosine was synthesized essentially as described by Migawa[32] (Scheme 1). Selective electrophilic fluorination of 6-chloro-7-deazapurine with the reagent Selectfluor afforded **1**, which was coupled to 1-*O*-acetyl-2,3,5-tri-*O*-benzoyl-*β*-D-ribofuranose to produce the protected nucleoside **2**. Simultaneous deprotection and aromatic substitution in methanolic ammonia provided **3** in addition to the methoxide substituted product in a ratio of 2:1. A similar coupling strategy with 6-chloro-7-deazaguanine did not produce the desired protected nucleoside, starting from either the unprotected or acetyl protected base. We turned instead to a nucleobase-anion glycosylation strategy[33,34] to obtain **4**, which was converted to **5** with aqueous ammonia (Scheme 2). Diazotation of **5** in the presence of HF produced 2-fluoro-7-deaza-adenosine, **6**, in low yield (the efficiency of this transformation is variable and dependent on heterocycle substitution patterns[35−37]). 2-Fluoro-adenosine is available from commercial

(28) Jones, F. D.; Ryder, S. P.; Strobel, S. A. *Nucleic Acids Res.* **2001**, *29*, 5115–5120.
(29) Zhao, Z. Y.; McLeod, A.; Harusawa, S.; Araki, L.; Yamaguchi, M.; Kurihara, T.; Lilley, D. M. J. *J. Am. Chem. Soc.* **2005**, *127*, 5026–5027.
(30) Wilson, T. J.; McLeod, A. C.; Lilley, D. M. J. *EMBO J.* **2007**, *26*, 2489–2500.
(31) Smith, M. D.; Collins, R. A. *Proc. Natl. Acad. Sci. U.S.A.* **2007**, *104*, 5818–5823.
(32) Wang, X. J.; Seth, P. P.; Ranken, R.; Swayze, E. E.; Migawa, M. T. *Nucleosides, Nucleotides Nucleic Acids* **2004**, *23*, 161–170.
(33) Rosemeyer, H.; Seela, F. *Helv. Chim. Acta* **1988**, *71*, 1573–1585.
(34) Seela, F.; Soulimane, T.; Mersmann, K.; Jurgens, T. *Helv. Chim. Acta* **1990**, *73*, 1879–1887.
(35) Eldrup, A. B.; et al. *J. Med. Chem.* **2004**, *47*, 5284–5297.
(36) Liu, M. C.; Luo, M. Z.; Mozdziesz, D. E.; Sartorelli, A. C. *Nucleosides, Nucleotides Nucleic Acids* **2005**, *24*, 45–62.
(37) Krolikiewicz, K.; Vorbruggen, H. *Nucleosides Nucleotides* **1994**, *13*, 673–678.

Scheme 2[a]

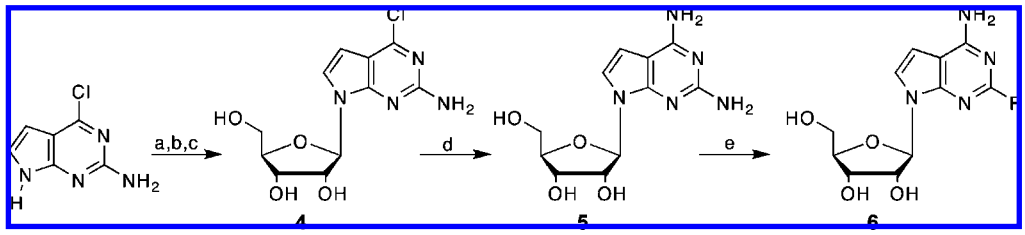

[a] (a) 5′-*O*-*tert*-Butyldimethylsilyl-2,3-*O*-isopropylidene-D-ribose, THF, CCl_4, $P(NMe_2)_3$, −72 °C 2 h. (b) 6-Chloro-7-deazaguanine, CH_3CN, KOH, TDA-1, product of (a) rt 20 h. (c) TFA, rt 50 min. (d) NH_3(aq), 75 °C 22 h. (e) HF/pyr, KNO_2, 0 °C 15 min.

Scheme 3[a]

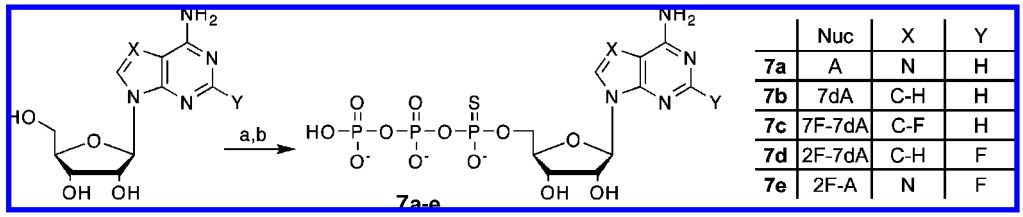

	Nuc	X	Y
7a	A	N	H
7b	7dA	C-H	H
7c	7F-7dA	C-F	H
7d	2F-7dA	C-H	F
7e	2F-A	N	F

[a] (a) $PSCl_3$, TEP, rt 1 h. (b) TBAP, TEP, rt 1 h.

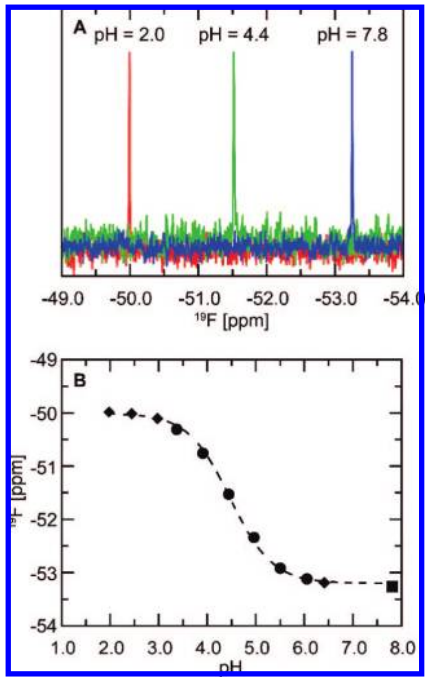

Figure 3. ^{19}F NMR titration of 7F-7dA. (A) ^{19}F NMR spectra referenced to internal fluorobenzene in 10% D_2O. (B) ^{19}F NMR frequency as a function of pH. A fit to a single ionization model (dashed line) provides a pK_a value of 4.5. pH was maintained with 100 mM phosphate (◆), citrate (●), or Tris (■) buffers.

sources. 5′-*O*-(1-Thio)nucleotide triphosphates were obtained from the corresponding nucleosides by the method of Frey[38] (Scheme 3) or from commercial sources (analogues **7a**,**7b**).

pK_a Values of Analogues. To determine the N1 pK_a values of the fluoro-adenosine analogues we recorded the ^{19}F NMR signal of analogue nucleosides as a function of pH in aqueous solutions. The ^{19}F NMR titration of 7F-7dA (Figure 3A) produces a titration curve that fits well to a single ionization model (Figure 3B). This fit yields a pK_a value of 4.5, which lies between that of A (pK_a = 3.5) and 7dA (pK_a = 5.2) as expected. ^{19}F NMR titrations were also performed for 2F-A and 2F-7dA. Neither of these analogues showed substantial frequency shifts within easily buffered pH ranges. However, titrations conducted with aqueous solutions of sulfuric acid provided completed titration curves for both 2F-A and 2F-7dA by 20 wt % H_2SO_4, with large ^{19}F frequency shifts (+4.7 ppm for 2F-A and −10.2 ppm for 2F-7dA). A combination of ^{19}F, ^{15}N, and ^{13}C NMR data confirmed that the site of protonation for 7F-7dA and 2F-7dA is N1, while the most basic site of 2F-A is N7 (see Supporting Information). Because 2F-A and 2F-7dA are protonated at different sites we report an upper limit for N1 pK_a values for these analogues of 1.0 (Figure 1).

Incorporation of Analogues by T7 RNA Polymerase. To test the ability of T7 RNA polymerase to incorporate analogues **7c**−**7e** we performed transcriptions with variable concentrations of these analogues and compared the incorporation level to transcriptions containing 0.05 mM 5′-*O*-(1-thio)adenosine triphosphates, **7a**. Transcriptions using EarI cut pHHVS as template and variable concentrations of individual analogues were purified, 5′-end labeled, and iodine cleaved (see Experimental Section). The products of iodine cleavage were separated by gel electrophoresis, and incorporation levels were determined by quantitating band intensities (data not shown). These results provided the analogue concentrations required to match the incorporation levels seen with **7a** (Table 1). The analogue concentrations in Table 1 were used in all subsequent transcriptions for production of VSE RNA. It has been previously shown that 7dA is incorporated with the same efficiency as A,[19] and we find 7F-7dA is similarly efficient, while fluorine substitutions at the 2-position of adenosine (2F-A) or 7-deaza-adenosine (2F-7dA) require slightly higher analogue concentrations. In addition to high incorporation efficiency, NAIM experiments require relatively even incorporation at all coded sites and minimal misincorporation. The intensity of iodine cleavage bands from unselected pools of unligated VSE RNA shows even incorporation with no evidence of misincorporation (Figure 4B,D), allowing the entire series to be used for NAIM studies.

VSE Ribozyme Interference Mapping. The functional consequence of analogue substitution at individual sites of the VSE

(38) Arabshahi, A.; Frey, P. A. *Biochem. Biophys. Res. Commun.* **1994**, *204*, 150–155.

Table 1. Analogue Concentrations Required for 5% Incorporation Level

analogue	analogue concn (mM)[a]	ATP concn (mM)
A	0.05	1.0
7dA	0.05	1.0
7F-7dA	0.05	1.0
2F-7dA	0.20	1.0
2F-A	0.20	1.0

[a] Concentrations are of Sp diasteriomers of 5′-*O*-(1-thio)nucleotide triphosphates. A and 7dA were added to reactions as pure Sp diasteriomers, while remaining analogues were added as 50:50 mixtures of diasteriomers. See Experimental Section for transcription details.

ribozyme was investigated by performing a ligation selection (see Experimental Section). Five unligated VSE RNA transcripts (NT 621−791, Figure 2), each containing one of the analogues **7a**−**7e** randomly incorporated at an ∼5% incorporation level, were incubated with a 5′-end labeled substrate (NT 599−620, Figure 2). This substrate RNA was constructed with a 2′,3′-cyclic phosphate at its 3′ terminus, as required for VSE ligation. Ligation reactions were allowed to proceed to ∼10% completion and then run on PAGE sequencing gels with or without iodine cleavage. Because only functional VSE transcripts are capable of ligating the substrate, the band intensities from the iodine cleaved selection report on the ability of an analogue to promote the ligation reaction when incorporated at a particular site. An increased band intensity relative to an unselected control corresponds to an enhancement in activity, while a decrease in band intensity corresponds to interference at that site.

NAIM sequencing gels typically resolved 36 of the 48 VSE adenosine positions, including all positions in the core of the ribozyme (Figures 4A,C). Only three of these sites, A698, A712, and A756, show interference with any analogue. The strongest of these interferences are easily identified from the sequencing gels directly by comparing band intensities from the VSE ligation selection experiment (Figure 4A,C) to the band intensities from 5′-end labeled unselected controls (Figure 4B,D). Interferences were further quantitated by drawing line profiles through the lanes, measuring the area of each band, and calculating interference (κ) or enhancement ($1/\kappa$) values for each position (see Experimental Section). A plot of average interference and enhancement values for each analogue at each site shows a selective and reproducible interference pattern for A698, A712, and A756, with very little effect at other sites (Figures 5). None of the sites of interference is paired in the predicted secondary structure of the VS ribozyme, and each has been shown to be critical to function by mutagenesis studies.[39−41]

Discussion

Attributes of Fluoro-Adenosine Analogues. Analogues **7a**−**7e** produce the largest span of N1 pK_a values of any adenosine series employed in NAIM studies to date, with the N1 pK_a values of 2F-A and 2F-7dA at least a full unit below that of any previously reported analogue.[21,23] Despite this dramatic range of pK_a values the minimal structural perturbation introduced by fluorine substitution allows this series to be introduced by transcription more readily and evenly than previous low pK_a analogues, while producing a more selective interference pattern. This finding is consistent with the observation that the normal triphosphate of 2F-A can be readily incorporated by *in vitro* transcription and that RNA duplexes containing this modification are only modestly destabilized.[42] A NAIM approach is particularly attractive for 2F-A since fluorine is readily displaced from this analogue under standard oligonucleotide synthesis deprotection conditions, making its introduction by chemical synthesis challenging.[43] In contrast 7F-7dA is stable under nucleophilic substitution conditions (Scheme 1) and could be incorporated site specifically via chemical synthesis. The large ^{19}F frequency shift observed between protonated and neutral forms (Figure 3) suggests this analogue may be useful as a spectroscopic reporter of adenosine protonation in folded RNA, as has been demonstrated for 5-fluoro-uracil.[44,45]

NAIM Results and Proposed VS Ribozyme Mechanism. Since the original report of VS ribozyme cleavage activity[46] a large body of kinetic and low resolution structural data has been collected. Extensive mutagenesis throughout the core of the ribozyme,[41,47] as well as in the substrate of a trans cleaving construct,[30] has identified two nucleotides critical for cleavage activity, G638 and A756. Although A756 is far from the cleavage site in primary sequence or secondary structure, UV cross-linking experiments place it near the scissile bond in the folded ribozyme,[48] supporting its potential catalytic role. A number of base modifications have been introduced at A756 by reassembling a three-piece construct, with significant reductions in activity found for modifications that alter the Watson−Crick face of the base.[49] Introduction of an imidazole nucleotide at A756 also supports cleavage, though at a greatly reduced rate, suggesting the ability to conduct proton transfer may be the key feature of this catalytic residue.[50] These data, combined with the pH dependent rates observed for the fastest known constructs,[30,31] and the lack of a divalent metal requirement[7] have led to a proposed general acid−base mechanism for VS ribozyme catalysis, with G638 and A756 as the sites of proton transfer.[30]

We conducted a NAIM study to test the proposed general acid−base mechanism of the VS ribozyme in the direction of ligation, with particular interest in the interference pattern at A756. If A756 is a site of proton transfer in the reaction, then reduced pK_a analogues would be expected to reduce activity when substituted at A756, either because of their reduced N1 nitrogen basicity (A756 as general base) or because of their reduced probability of being protonated at neutral pH (A756 as general acid).[51] Because some chemical modification is required to perturb pK_a values, the effect of modifications unrelated to pK_a shifts is a concern. For this reason the close structural similarity between analogues **7a**−**7e** aids greatly in the interpretation of their interference patterns.

(39) Rastogi, T.; Beattie, T. L.; Olive, J. E.; Collins, R. A. *EMBO J.* **1996**, *15*, 2820–2825.
(40) Sood, V. D.; Collins, R. A. *J. Mol. Biol.* **2001**, *313*, 1013–1019.
(41) Lafontaine, D. A.; Wilson, T. J.; Norman, D. G.; Lilley, D. M. J. *J. Mol. Biol.* **2001**, *312*, 663–674.
(42) Scott, L. G.; Geierstanger, B. H.; Williamson, J. R.; Hennig, M. *J. Am. Chem. Soc.* **2004**, *126*, 11776–11777.
(43) Peng, X. H.; Li, H.; Seela, F. *Nucleic Acids Res.* **2006**, *34*, 5987–6000.
(44) Sowers, L. C.; Eritja, R.; Kaplan, B.; Goodman, M. F.; Fazakerly, G. V. *J. Biol. Chem.* **1988**, *263*, 14794–14801.
(45) Hardin, C. C.; Gollnick, P.; Kallenbach, N. R.; Cohn, M.; Horowitz, J. *Biochemistry* **1986**, *25*, 5699–5709.
(46) Saville, B. J.; Collins, R. A. *Cell* **1990**, *61*, 685–696.
(47) Sood, V. D.; Collins, R. A. *J. Mol. Biol.* **2002**, *320*, 443–454.
(48) Hiley, S. L.; Sood, V. D.; Fan, J.; Collins, R. A. *EMBO J.* **2002**, *21*, 4691–4698.
(49) Lafontaine, D. A.; Wilson, T. J.; Zhao, Z. Y.; Lilley, D. M. J. *J. Mol. Biol.* **2002**, *323*, 23–34.
(50) Lilley, D. M. J. *Biol. Chem.* **2007**, *388*, 699–704.
(51) Bevilacqua, P. C. *Biochemistry* **2003**, *42*, 2259–2265.

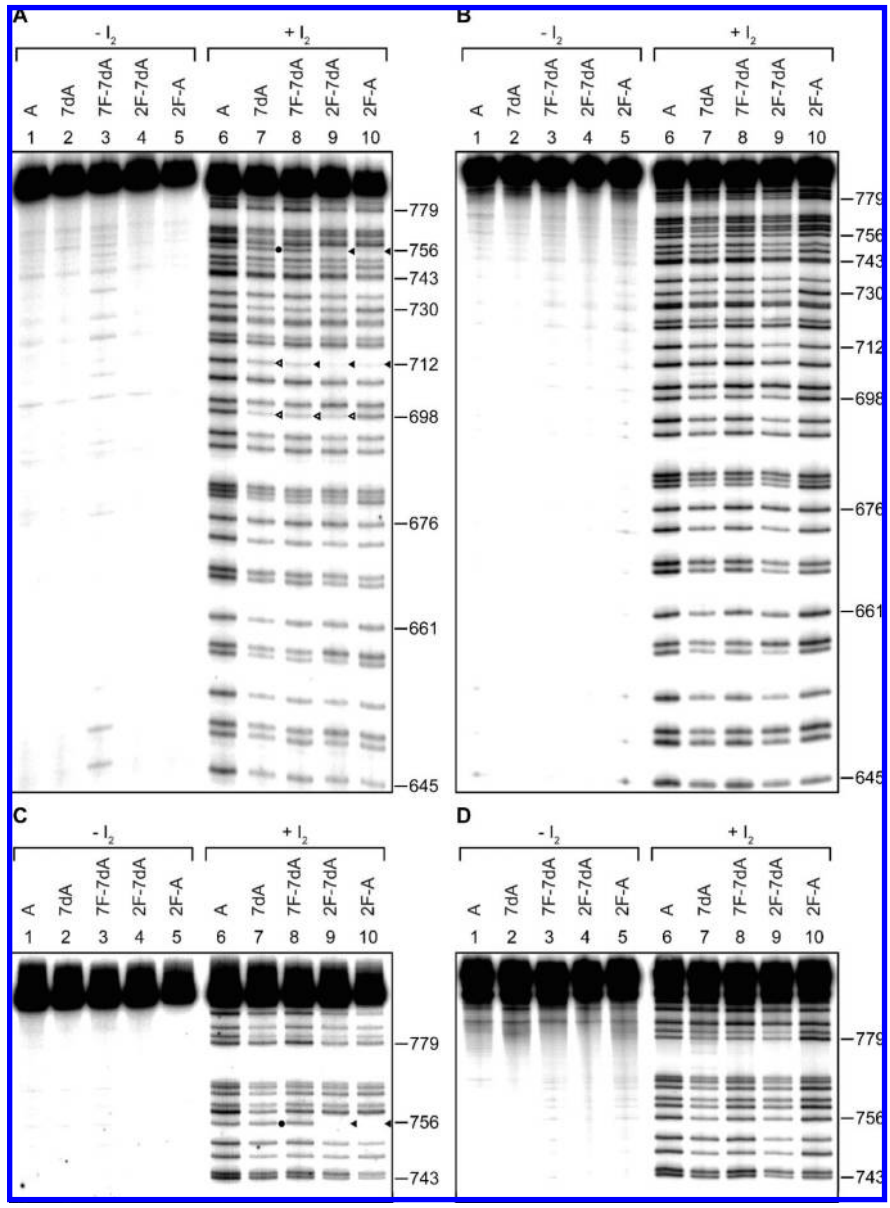

Figure 4. (A,C) Sequencing gel of NAIM ligation selections run for sufficient times to resolve short (A) or long (C) iodine cleavage products. Ligation products were treated with iodine (lanes 6−10) or without iodine (lanes 1−5) prior to being loaded onto the gel. The analogue incorporated for each selection is shown above lanes, and nucleotide positions are shown to the right. Sites of modified activity are marked as follows: strong interference ($\kappa >$ 4) filled triangle, modest interference ($4 > \kappa > 2$) open triangle, enhancement ($1/\kappa > 2$) filled circle. (B,D) Sequencing gel of 5′-end labeled unligated VSE RNAs labeled as above, run to control for level of analogue incorporation.

The effect of analogue substitution at A756 (Figure 5A−D) ranges from significant enhancement (7dA) to strong interference (2F-7dA and 2F-A). The enhancement observed for 7dA, a pK_a elevated base, is reduced when the 7-fluoro substitution is introduced, presumably because 7F-7dA moves the N1 pK_a back toward that of A. The enhancement observed for 7dA is unlikely to originate from the loss of N7 because 2F-7dA shows strong interference. For the pK_a reduced analogues the interference observed for 2F-A is greater than that of 2F-7dA, indicative of a pK_a effect since 2F-A is expected to have the lower N1 pK_a (see Supporting Information). A756 is the only site that shows an interference pattern directly related to N1 pK_a, and this pattern of interference suggests protonation at this site is required for VSE function.

In addition to the pK_a dependent interference observed at A756, analogues **7b**−**7e** also produced interferences at two important structural positions, A698 and A712. The interference pattern observed at both sites supports proposed uridine turns, defined by the consensus sequence U−N−R (where N is any nucleotide and R is a purine). The structure of canonical uridine turns includes a key hydrogen bond between the 2′-hydroxyl of the U and the N7 of the purine.[52] Consistent with the proposed U696−G697−A698 uridine turn interference at A698 results from the loss of N7 (7dA, 7F-7dA, 2F-7dA) and is independent of the N1 pK_a, as demonstrated by the lack of interference for 2F-A (Figure 5). This pattern supports a long-range pseudoknot between helices I and V built in part from a uridine turn involving A698.[39] These interferences also confirm

(52) Quigley, G. J.; Rich, A. *Science* **1976**, *194*, 796–806.

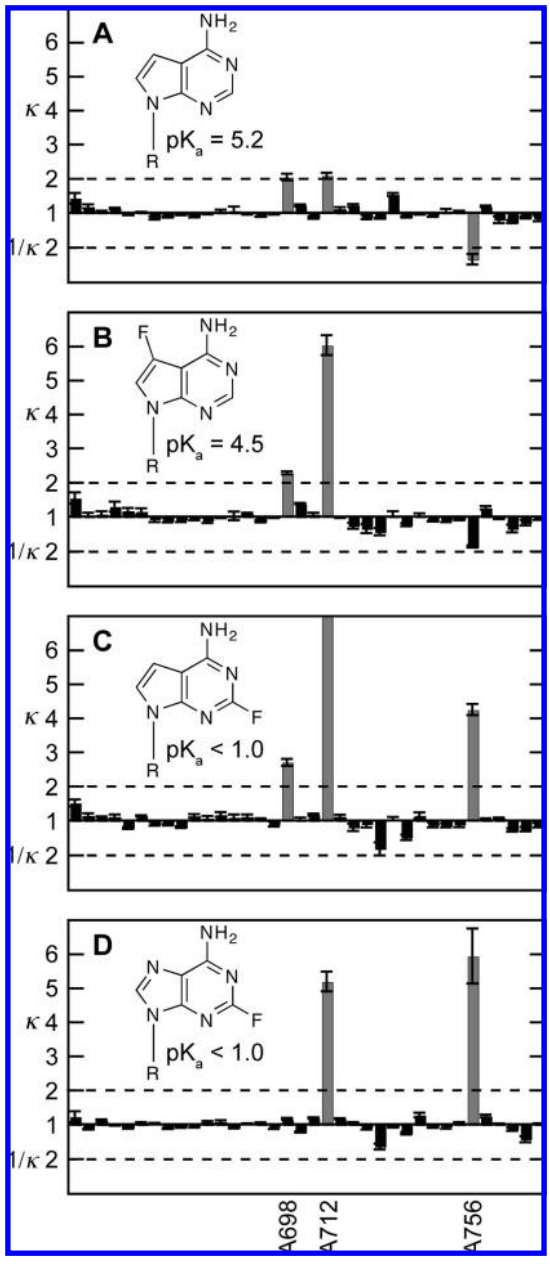

Figure 5. Calculated interference (κ) or enhancement ($1/\kappa$) values for adenosine analogues 7dA (A), 7F-7dA (B), 2F-7dA (C), and 2F-A (D). Values are provided for adenosine sites A645 (left) to A767 (right) and represent the average of four measurements with standard deviation error bars. Interferences or enhancements greater than 2 (dashed line) are considered significant and shaded gray.

the functional relevance of the uridine turn observed in the NMR structure of VS nucleotides 693−702.[53]

The interference pattern at A712 is less clearly interpretable, in part because significant interference has been observed with nearly every analogue tested to date.[21] A uridine turn has also been proposed for residues U710−G711−A712 based on mutagenesis and chemical modification protection,[40] and the interferences observed for analogues lacking N7 are consistent with that prediction. However, in contrast to A698, which can be replaced with G in the context of the U631C/A698G double mutant, the A712G mutant is inactive, suggesting an additional interaction with this base or very tight packing at this position. Although the origin of base selectivity at A712 in the native sequence is unclear, it is known that this site is not directly involved in catalysis since residues 710−712 can be replaced with hairpins of various length and sequence with modest decreases in rate.[40]

The current model for VS ribozyme catalysis employs A756 as a general acid or general base, with some other functional group, possibly G638, as the complementary site of proton transfer[30] (Figure 6). The interference pattern observed with the fluoro-adenosine analogues of this study strongly supports a functional role of A756 protonation, as this is the only site in the ribozyme that shows a pK_a dependent interference pattern. However, the interference pattern itself can neither distinguish between a potential general acid or general base role for A756 nor preclude a structural role for the protonated form of A756.[51] One approach to resolve this ambiguity is structural studies. Although there are no atomic structures yet available for the VS ribozyme, it has been suggested[30] that the VS may position functional groups in a manner similar to the Hairpin ribozyme, which places a G at the 2′-oxygen and an A near the 5′-hydroxyl.[54] In this scenario A756 would act as the general base in the ligation reaction (Figure 6B), and interferences caused by low pK_a analogues such as 2F-A would arise from the analogue's reduced N1 basicity. This dependence on the active site adenosine N1 pK_a would be analogous to that observed in the Hairpin ribozyme, where rescue of the A38 abasic substitution shows a strong dependence on the exogenous nucleobase pK_a.[55]

Conclusions

The fluoro-adenosine analogues presented in this study provide an improved series to determine sites of adenosine protonation by NAIM analysis. These analogues have N1 pK_a values spanning more than 4 pK_a units while maintaining a normal Watson−Crick hydrogen bonding face and introducing minimal steric perturbation. Each of the analogues is evenly incorporated by T7 RNA polymerase with good fidelity at relatively low analogue concentrations. A NAIM analysis carried out on a ligating form of the VS ribozyme led to three sites of interference and a single site, A756, whose interference pattern is consistent with functional protonation. The small number of interferences observed demonstrates the ability of this new series to produce extremely selective interference patterns. Because the entire series is related by minor chemical modifications, interferences not originating from N1 pK_a perturbations are readily controlled for. In addition to its use in activity studies we anticipate 7F-7dA may find use as a spectroscopic probe of pK_a values because of its moderate pK_a, large ^{19}F NMR frequency shift upon protonation, and ease of incorporation.

Experimental Section

Synthesis. Reagents: 2-Fluoro-adenosine (SynQuest), 6-chloro-7-deazapurine, 6-chloro-7-deazaguanine, and 5′-*O*-*tert*-butyldimethylsilyl-2,3-*O*-isopropylidene-D-ribose (Toronto Research Chemicals), 1-*O*-acetyl-2,3,5-tri-*O*-benzoyl-β-D-ribofuranose (Acros Organics), NMR solvents (Cambridge Isotopes), all remaining reagents, and solvents (Sigma-Aldrich). Instrumentation: ^{1}H NMR (Bruker, 400 or 500 MHz), ^{19}F NMR and ^{31}P NMR (Bruker, 400

(53) Campbell, D. O.; Bouchard, P.; Desjardins, G.; Legault, P. *Biochemistry* **2006**, *45*, 10591–10605.
(54) Salter, J.; Krucinska, J.; Alam, S.; Grum-Tokars, V.; Wedekind, J. E. *Biochemistry* **2006**, *45*, 686–700.
(55) Kuzmin, Y. I.; Da Costa, C. P.; Cottrell, J. W.; Fedor, M. J. *J. Mol. Biol.* **2005**, *349*, 989–1010.

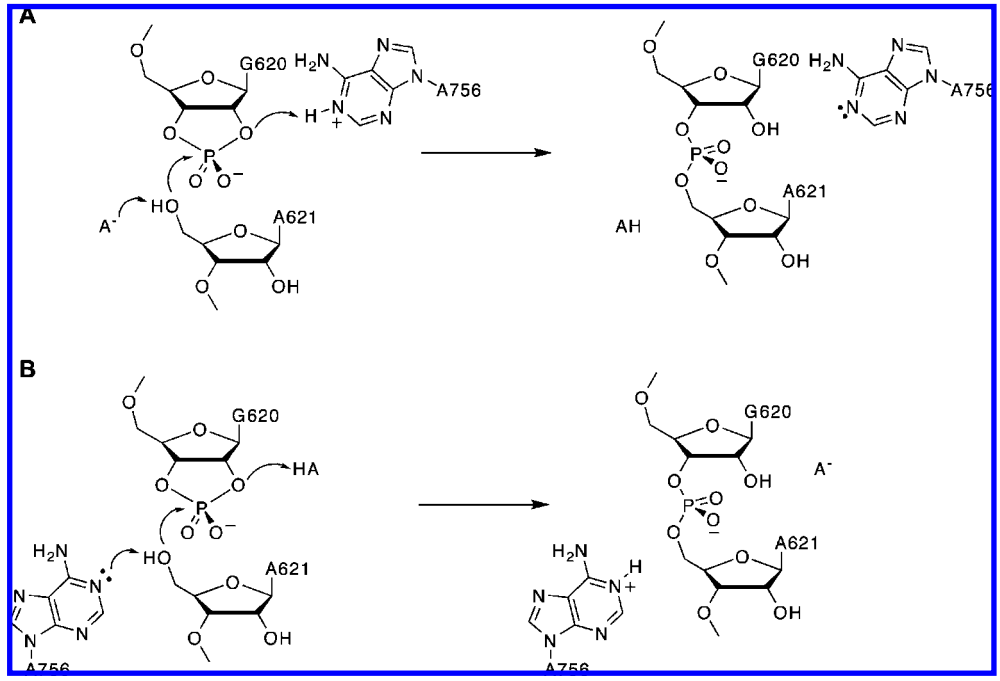

Figure 6. Two potential catalytic roles for A756 protonation. In a general acid/base mechanism A756 could act as either the general acid (A) or general base (B) in the ligation reaction, with another ionizable group, HA, as the complementary site of proton transfer.

MHz), MS (Waters, Micromass ZQ), high pressure bomb (Parr Instruments, bomb number 4745), FPLC (Amersham, AKTAprime), anion exchange column (GE Healthcare, HiTrap Q HP).

4-Chloro-5-fluoro-7*H*-pyrrolo[2,3-*d*]pyrimidine (1). 6-Chloro-7-deazapurine (258 mg, 1.7 mmol) was dried by coevaporation of pyridine (5 mL × 3) and placed under vacuum overnight. Selectfluor (890 mg, 2.5 mmol) was added followed by anhydrous acetonitrile (12.5 mL) and acetic acid (2.5 mL). The solution was refluxed at 70 °C under Ar for 15 h and cooled to rt. Solvent was removed under reduced pressure and coevaporated with toluene (5 mL × 2) to leave a brown solid. A suspension of this solid in 1:1 DCM/EtOAc (10 mL) was filtered through 1 cm of silica, which was washed with 1:1 DCM/EtOAc (150 mL). Evaporation of washes left a yellow solid that was purified on a silica column with DCM/EtOAc (4:1) to give 125 mg (43% yield) of **1** as a white solid. $R_f = 0.32$ (1:1 DCM/EtOAc). ^{1}H NMR (DMSO-d_6) δ 12.47 (br s, 1H), 8.61 (s, 1H), 7.71 (d, 1H, $J = 2.2$ Hz); ^{19}F NMR (DMSO-d_6) δ −170.75 (d, $J = 2.2$ Hz). MS expected $(M + H)^+ = 172.0$, observed 171.9 $(M + H)^+$.

4-Chloro-5-fluoro-7-(2,3,5-tri-*O*-benzoyl-β-D-ribofuranosyl)pyrrolo[2,3-*d*]pyrimidine (2). In separate round bottom flasks 4-chloro-5-fluoro-7*H*-pyrrolo[2,3-*d*]pyrimidine (**1**) (125 mg, 0.73 mmol) and 1-*O*-acetyl-2,3,5-tri-*O*-benzoyl-β-D-ribofuranose (400 mg, 0.79 mmol) were coevaporated with acetonitrile and dried under vacuum overnight. To a suspension of 4-chloro-5-fluoro-7*H*-pyrrolo[2,3-*d*]pyrimidine in anhydrous acetonitrile (3.0 mL) was added *N*,*O*-bis(trimethylsilyl)acetamide (0.21 mL, 0.82 mmol), to form a clear slightly purple solution. 1-*O*-Acetyl-2,3,5-tri-*O*-benzoyl-β-D-ribofuranose was dissolved in anhydrous acetonitrile (1.6 mL) with mild heating and added to the reaction, followed by trimethylsily trifluoromethanesulfonate (0.14 mL, 0.79 mmol) dropwise to produce a clear yellow solution. The reaction was stirred at rt for 15 min and then refluxed at 80 °C for 1 h. The orange/brown reaction was cooled to rt, diluted with EtOAc (25 mL), and washed with sat. $NaHCO_3$ (25 mL) and sat. NaCl (25 mL), then dried over $MgSO_4$, and concentrated to give a yellow oil. Purification by silica column with 10−25% EtOAc in hexanes gave **2** (150 mg, 33% yield) as a yellow/white foam. $R_f = 0.33$ (30% EtOAc in hexanes). ^{1}H NMR ($CDCl_3$) δ 8.57 (s, 1H), 8.10 (d, 2H, $J = 7.1$ Hz), 7.98 (d, 2H, $J = 7.1$ Hz), 7.89(d, 2H, $J = 7.1$ Hz), 7.60−7.32 (m, 9H), 7.15 (d, 1H, $J = 2.5$ Hz), 6.68 (d, 1H, $J = 2.8$ Hz), 6.11 (m, 1H), 6.05 (m, 1H), 4.85 (m, 1H), 4.76 (m, 1H), 4.65 (m, 1H). ^{19}F NMR ($CDCl_3$) δ −165.80 (s). MS expected $(M + H)^+ = 616.1$, observed 616.3 $(M + H)^+$, 638.1 $(M + Na)^+$.

7-Fluoro-7-deaza-adenosine (3). 4-Chloro-5-fluoro-7-(2,3,5-tri-*O*-benzoyl-β-D-ribofuranosyl) pyrrolo[2,3-*d*]pyrimidine (2) (150 mg, 0.24 mmol) was dried under vacuum overnight in a round bottom flask and then cooled to 0 °C under Ar. A 7 N solution of ammonia in MeOH (10.0 mL) was added, and the solution was stirred at 0 °C until a clear solution formed. This solution was transferred to the Teflon insert of a stainless steel bomb and heated to 73 °C for 18 h. After cooling the solvent was removed to leave a yellow solid that was coevaporated with MeOH (20 mL × 3). Purification by a silica column with 5−15% MeOH in DCM gave **3** (27 mg, 38% yield) as a white solid. $R_f = 0.23$ (15% MeOH in DCM). ^{1}H NMR (DMSO-d_6) δ 8.05 (s, 1H), 7.34 (d, 1H, $J = 1.9$ Hz), 7.00 (br s, 2H), 6.05 (m, 1H) 5.35 (d, 1H, $J = 5.8$ Hz), 5.14 (m, 2H), 4.27 (m, 1H), 4.04 (m, 1H), 3.85 (m, 1H), 3.61−3.47 (m, 2H). ^{19}F NMR (DMSO-d_6) δ −167.73 (s). MS expected $(M + H)^+ = 285.1$, observed 285.1 $(M + H)^+$, 307.1 $(M + Na)^+$.

4-Chloro-7-(β-D-ribofuranosyl)-7*H*-pyrrolo[2,3-*d*]pyrimidin-2-amine (4). Compound **4** was synthesized in three steps by the method of Seela.[33,34,56] (a) Synthesis of 5′-*O*-*tert*-butyldimethylsilyl-2,3-*O*-isopropylidene-D-ribose chloride: 5′-*O*-*tert*-butyldimethylsilyl-2,3-*O*-isopropylidene-D-ribose (1.36 g, 4.47 mmol) was dried under vacuum overnight and placed under Ar. Anhydrous THF (14.0 mL) and CCl_4 (0.52 mL) were added, and the solution was cooled to −72 °C. To the cooled solution tris(dimethylamino)phosphane (0.83 mL, 4.57 mmol) was added dropwise over 15 min and stirred for 2 h with brief periods of slight warming to prevent gel formation. The reaction was concentrated to 4.5 mL and used immediately without purification in the following step. (b) Nucleobase-anion glycosylation: In separate flasks 6-chloro-7-deazaguanine (733 mg, 4.35 mmol) and powdered potassium hydroxide (760 mg, 13.5 mmol) were dried under vacuum overnight. Anhydrous acetonitrile (36.0 mL) was added to the potassium hydroxide, followed by tris[2-(2-methoxyethoxy)ethyl]-amine (0.028 mL) and stirred for 10 min at rt. 6-Chloro-7-

(56) Wilcox, C. S.; Otoski, R. M. *Tetrahedron Lett.* **1986**, *27*, 1011–1014.

deazaguanine was added and stirred for 10 min at rt to produce a clear yellow solution. To this solution the crude THF solution of 5′-*O*-*tert*-butyldimethylsilyl-2,3-*O*-isopropylidene-D-ribose chloride from the previous step was added and stirred at rt for 20 h, changing in color from light pink to dark brown. Insoluble material was filtered off, and the concentrated filtrate was purified on a silica column with 20% EtOAc in hexanes to provide the protected nucleoside (R_f = 0.24, 20% EtOAc in hexanes). (c) Nucleoside deprotection: To the protected nucleoside of the previous step was added 90% aqueous trifluoroacetic acid (3.7 mL), and the reaction stirred at rt for 50 min. The reaction was concentrated under reduced pressure and coevaporated with MeOH (10 mL × 5). Purification by silica column with 10% MeOH in DCM gave **4** (350 mg, 27% overall yield) as a white solid. R_f = 0.23 (10% MeOH in DCM). ^{1}H NMR (DMSO-d_6) δ 7.37 (d, 1H, J = 3.8 Hz), 6.69 (br s, 1H), 6.36 (d, 1H, J = 3.8 Hz), 5.97 (d, 1H, J = 6.3 Hz), 5.28 (d, 1H, J = 6.2 Hz), 5.08 (d, 1H, J = 4.6 Hz), 4.97 (t, 1H, J = 5.4 Hz), 4.29 (m, 1H), 4.04 (m, 1H), 3.83 (m, 1H), 3.57−3.50 (m, 2H). MS expected $(M + H)^+$ =301.1, observed 301.1 $(M + H)^+$, 323.2 $(M + Na)^+$.

7-(β-D-ribofuranosyl)-7*H*-pyrrolo[2,3-*d*]pyrimidin-2,4-diamine (5). 4-Chloro-7-(β-D-ribofuranosyl)-7*H*-pyrrolo[2,3-*d*]pyrimidin-2-amine (**4**) (250 mg, 0.83 mmol) was transferred to the Teflon insert of a steel bomb, and 30% aqueous ammonia (15 mL) was added. The reaction was heated to 75 °C for 22 h, cooled, and evaporated to dryness. Purification by silica column with 40% MeOH in DCM gave **5** (211 mg, 90% yield) as a white solid. R_f = 0.49 (40% MeOH in DCM). ^{1}H NMR (DMSO-d_6) δ 6.87 (d, 1H, J = 3.6 Hz), 6.57 (br s, 2H), 6.35 (d, 1H, J = 3.6 Hz), 5.82 (d, 1H, J = 6.4 Hz), 5.49 (br s, 2H), 5.33 (br s, 1H), 5.16 (d, 1H, J = 6.3 Hz), 5.00 (d, 1H, J = 4.5 Hz), 4.32 (m, 1H), 4.10 (m, 1H), 4.02 (m, 1H), 3.81 (m, 1H), 3.57−3.46 (m, 2H). MS expected $(M + H)^+$ = 282.1, observed 282.1 $(M + H)^+$, 304.0 $(M + Na)^+$.

2-Fluoro-7-deaza-adenosine (6). 7-(β-D-ribofuranosyl)-7*H*-pyrrolo[2,3-*d*]pyrimidin-2,4-diamine (**5**) (211 mg, 0.75 mmol) was transferred to a polypropylene tube with anhydrous pyridine (0.4 mL). To a stirred suspension cooled to 0 °C, 70% hydrogen fluoride in pyridine (0.67 mL) was added. Potassium nitrite (80 mg, 0.94 mmol) dissolved in water (0.16 mL) was then added slowly to the stirred reaction, leading to evolution of gas and a green color. After 15 min at 0 °C the reaction was poured into a stirred suspension of calcium carbonate (1.7 g) in water (3.0 mL). The slurry was stirred at 0 °C for 2 h, warmed to rt and stirred for 18 h, and then filtered to give a red/brown solution. The insoluble material was washed with water (2.0 mL) and 1:1 water/EtOH (2.0 mL × 2), concentrated, and coevaporated with toluene (10 mL × 3). Purification by silica column with 20% MeOH in DCM gave **6** (23 mg, 11% yield) as a white solid. R_f = 0.34 (20% MeOH in DCM). ^{1}H NMR (DMSO-d_6) δ 7.54 (br s, 2H), 7.31 (d, 1H, J = 3.7 Hz), 6.60 (d, 1H, J = 3.7 Hz), 5.87 (d, 1H, J = 6.2 Hz), 5.27 (d, 1H, J = 6.5 Hz), 5.10 (d, 1H, J = 4.9 Hz), 4.99 (t, 1H, J = 5.5 Hz), 4.31 (m, 1H), 4.04 (m, 1H), 3.85 (m, 1H), 3.63−3.46 (m, 2H). MS expected $(M + H)^+$ =285.1, observed 285.1 $(M + H)^+$, 307.0 $(M + Na)^+$. ^{19}F NMR (DMSO-d_6) δ −53.84 (s).

5′-*O*-(1-Thio)nucleotide triphosphates (7c−7e). Representative procedure: The nucleoside (0.0095 mmol) was dried by coevaporation with pyridine (1.0 mL × 3), put under high vacuum overnight, dissolved in triethyl phosphate (0.5 mL) with gentle heating, and cooled to rt under Ar. To this solution trioctylamine (0.062 mL, 0.014 mmol) was added, followed by thiophosphoryl chloride (0.014 mL, 0.014 mmol), and the reaction was stirred at rt for 1 h. Dried tributylammonium pyrophosphate (250 mg, 0.055 mmol) was dissolved in triethyl phosphate (2.0 mL) with heating, cooled, added to the reaction, and the reaction stirred for 1 h at rt. To the stirred reaction triethyl amine (0.8 mL) was added, precipitating a white solid that was collected by centrifugation. The precipitate was dissolved in triethyl amine bicarbonate buffer (TEAB, 5.0 mL, 50 mM pH = 8.0) and incubated at rt for 12 h. The crude product, containing mono-, di-, tri-, tetra-, and pentaphosphates, was filtered and applied to a HiTrap Q HP anion exchange column and eluted with a linear gradient of TEAB (0.05−1.0 M). Purification of analogue triphosphates by anion exchange column chromatography yielded a 50:50 mixture of Rp and Sp diasteriomers, as determined by ^{31}P NMR. Triphosphate, cyclic triphosphate, and (1-thio) cyclic triphosphate coeluted with analogue triphosphates in some preparations and were observed in the mass spectra and ^{31}P NMR spectra of these samples. No effort was made to eliminate these impurities as they did not interfere with subsequent transcriptions. (**7c**) ^{31}P NMR (10% D_2O) δ 42.69 (m, 1P), −6.55 (d, 1P, J = 20.2 Hz), −23.07 to −23.42 (m, 1P). ^{19}F NMR (10% D_2O) δ −166.16 (d, J = 42.9 Hz). MS expected $(M)^-$ = 538.9, observed 539.4 $(M)^-$. (**7d**) ^{31}P NMR (10% D_2O) δ 42.61 (m, 1P), −7.35 (d, 1P, J = 19.8 Hz), −23.45 to −23.80 (m, 1P). ^{19}F NMR (10% D_2O) δ −55.78 (s). MS expected $(M)^-$ = 538.9, observed 539.1 $(M)^-$. (**7e**) ^{31}P NMR (10% D_2O) δ 42.71 (m), −6.67 (d, 1P, J = 19.8 Hz), −23.16 to −23.51 (m, 1P). ^{19}F NMR (10% D_2O) δ −52.92 (s). MS expected $(M)^-$ = 539.9, observed 540.0 $(M)^-$.

^{19}F NMR Titrations. Nucleosides were dissolved in 10% D_2O solutions to a final concentration of ∼1.0 mM. The pH of each solution was set by either 100 mM buffer (from pH = 2.0 to 8.0) or by wt % H_2SO_4 solutions (Hammett acidity function[57] H_0 = −1.2 to 2.0). Fluorobenzene was included in each sample as an internal reference. ^{19}F NMR spectra were obtained, and peak positions were fit to the following single ionization model to yield pK_a values and frequency shifts:

$$F_{obs} = \frac{F_A + F_{HA}(10^{(pK_a - pH)})}{1 + 10^{(pK_a - pH)}}$$

where F_{obs} is the observed frequency, F_A is the frequency of the neutral nucleoside, and F_{HA} is the frequency of the protonated nucleoside.

Extinction Coefficients. Extinction coefficients for analogues **7c−7e** were estimated by obtaining UV−vis spectra of solutions of known concentration of the corresponding nucleosides in 100 mM phosphate buffer (pH = 7.0) (see Supporting Information) and yielded the following absorption maxima and extinction coefficients; 7F-7dA (278 nm, ε = 7700 M^{-1} cm^{-1}), 2F-7dA (269 nm, ε = 9200 M^{-1} cm^{-1}), 2F-A (262 nm, ε = 13 400 M^{-1} cm^{-1}). These extinction coefficients were used to calculate analogue concentrations for subsequent transcription reactions.

VSE RNA Transcription. Unligated VSE RNA (NT 621−791) was obtained by transcription of EarI cut pHHVS plasmid. This RNA contains two mutations to the native VS sequence, A782U and U785C, that increase ligation activity.[28] The pHHVS plasmid[21] contains a Hammerhead ribozyme upstream of the VSE sequence and an engineered EarI site at U791. Hammerhead processing during transcription produces a uniform 5′-hydroxyl at A621, which acts as the nucleophile in subsequent ligation selection. VSE transcriptions (100 μL) contained 40 mM Tris buffer (pH = 8.0), 10 mM $MgCl_2$, 2 mM spermidine, 5 mM DTT, 0.005% Triton X-100, 1 mM of each NTP, analogues **7a−7e** to reach concentrations in Table 1, 2 μg of EarI cut pHHVS, 1 unit of inorganic pyrophosphatase (Sigma) and T7 RNA polymerase to a final concentration of 0.1 mg/mL. Transcriptions were incubated for 2 h at 37 °C, which led to nearly complete Hammerhead processing following transcription. VSE RNA was purified by 8% denaturing PAGE and eluted at rt for 30 min with 10 mM Tris buffer (pH = 8.0), 0.1 mM EDTA, 250 mM NaCl, 2% w/w SDS. Elutions were PCA extracted and concentrated by ethanol precipitation, resuspended in $T_{10}E_{0.1}$ (Tris buffer (pH = 8.0), 0.1 mM EDTA), and stored at −20 °C. For 5′-end labeled controls unligated VSE RNAs were labeled with 5 mCi [γ-^{32}P] ATP (Perkin-Elmer) with T4 polynucleotide kinase (New England Biolabs) and purified as above.

(57) Albert, A.; Serjeant, E. P. *The Determination of Ionization Constants*, 3rd ed.; Chapman and Hall: New York, 1984.

Labeled samples were split into two aliquots, treated with iodine (1/10 volume of 100 mM iodine in ethanol) or ethanol alone, and run on 8% denaturing PAGE sequencing gels.

Ligation Substrate. The 22 NT substrate used for ligation selections corresponds to VS nucleotides 599−620. To produce the substrate with the required 2′,3′-cyclic phosphate terminus a trans-cleaving VS ribozyme (denoted Rz[58]) was used. First a 41 NT oligo corresponding to VS nucleotides 599−639 was synthesized (Dharmacon) and labeled with 5 mCi [γ-^{32}P] ATP (Perkin-Elmer) using T4 polynucleotide kinase (New England Biolabs). This oligo contains the stem I helix recognized by the trans-cleaving Rz ribozyme. Following the labeling reaction the solution was heated to 75 °C for 20 min to deactivate the kinase and cooled to 50 °C. Trans-cleavage buffer and Rz RNA were added to give the following final concentrations: 100 mM Tris Buffer (pH = 7.5), 25 mM KCl, 20 mM $MgCl_2$, 2 mM spermidine, 4 mM DTT, 2 μM Rz RNA, and 2 μM labeled 41 NT oligo. After slow cooling to 30 °C the trans-cleavage reaction was incubated at 30 °C for 1.5 h (this procedure typically provided >75% cleavage product). Residual [γ-^{32}P] ATP was removed with size exclusion columns (Microspin G-50, GE Healthcare), and the 22NT substrate was purified by 20% nondenaturing PAGE, eluted into $T_{10}E_{0.1}$, PCA extracted, and concentrated by ethanol precipitation.

NAIM Ligation Selections. Individual ligation reactions were performed with labeled 22NT substrate and unlabeled VSE RNAs. Each of the VSE RNAs contained one of the analogues **7a**−**7e** randomly incorporated at adenosine sites. VSE RNAs were incubated in 2× ligation buffer at 50 °C for 15 min and slowly cooled to 30 °C over 30 min. 22NT substrate was heated to 30 °C and added to reactions to give the following final concentrations in a volume of 10 μL; 50 mM Tris buffer (pH = 7.5), 5 mM $MgCl_2$, 25 mM KCl, 0.4 μM VSE RNA, 0.05 μM 22NT substrate. Reactions were incubated at 30 °C for 30−45 min which was sufficient time to produce 10−15% ligation. Reactions were quenched with 10 μL of formamide loading buffer and split into two aliquots. Iodine (1.0 μL of 100 mM in ethanol) was added to one aliquot to cleave phosphorothioate linkages, while the other aliquot was treated with ethanol alone to control for nonspecific cleavage. Cleaved and uncleaved samples were run on 8% denaturing PAGE sequencing gels. Because only active members of the VSE RNA pool become radiolabeled, separation of active and inactive members was unnecessary.

Interference Quantitation. Ligation selection gels and 5′-end labeled control gels were dried and exposed to phosphorimager screens. Interferences or enhancements in activity are recognized as decreases or increases in band intensity in the ligation selection gel (Figure 4A,C) relative to the unligated 5′-end labeled controls (Figure 4B,D). Because the phosphorothioate substitution can itself lead to changes in activity, a control for this substitution is needed, namely the parental analogue **7a** which introduces the backbone modification without nucleobase substitutions. If significant nonspecific degradation is observed the relative band intensities no longer report on sites of analogue incorporation. Iodine-free controls were run on the same gels to check for this possibility (Figure 4A−D, lanes 1−5). To quantitate sites of interference line profiles were drawn through ligation selection and control lanes and peak areas were calculated. From these peak areas an interference value, κ, is calculated[20]

$$\kappa = \mathrm{NF} \times \frac{(\mathrm{N\alpha Sligation}/\delta\alpha\mathrm{Sligation})}{(\mathrm{N\alpha S5'control}/\delta\alpha\mathrm{S5'control})} \qquad (2)$$

where each member of the fraction is the peak area for a particular site in the ligation or 5′-end labeled gel, NαS is the parental analogue **7a**, and δαS is one of the pK_a perturbed analogues (**7b**−**7e**). A normalization factor (NF) is calculated from the ratios to account for uneven loading of the lanes.[20] Interference values calculated in this way normalize both for the extent of analogue incorporation at a particular site and for the effect the phosphorothioate substitution at that site. Interference values between 0.5 and 2.0 are typically viewed as insignificant, while those below 0.5 are often expressed as 1/κ enhancements. For large interference values increasingly weak bands must be quantitated in the background of minor nonspecific degradation. Interference values above 6.0 are considered indistinguishable for this reason. Figure 5A−D provides the average of four interference values calculated for each of the analogues of this study. Because large iodine cleavage products were insufficiently resolved in some gels, interference values are reported for sites A645−A767.

Acknowledgment. We thank M. T. Migawa for guidance in the synthesis of 7F-7dA. This work was supported by NSF Grant MCB-0544255 and an NIH NRSA fellowship to I.T.S. (GM078764).

Supporting Information Available: Extinction spectra of compounds **7c**−**7e**; ^{19}F titrations for 7F-7dA, 2F-7dA, and 2F-A; ^{1}H−^{15}N HMBC spectra of A, 7F-7dA, and 2F-A in protonated and unprotonated form; ^{13}C chemical shifts for 7F-7dA, 2F-7dA, and 2F-A in protonated and unprotonated form; Complete ref 35. This material is available free of charge via the Internet at http://pubs.acs.org.

JA803336Y

(58) Guo, H. C. T.; Collins, R. A. *EMBO J.* **1995**, *14*, 368–376.